Templated Synthesis of Mesolamellar *n*-Alkylamine Borophosphates

Shuang Chen,[†,‡,§] Horst Borrmann,[§] Ya-Xi Huang,[||] Zhi-Jun Zhang,[†,‡] Hao-Hong Chen,[†] and Jing-Tai Zhao*,[†]

State Key Laboratory of High Performance Ceramics and Superfine Microstructure, Shanghai Institute of Ceramics, Chinese Academy of Sciences, Shanghai 200050, PR China, Graduate School of the Chinese Academy of Sciences, Beijing, PR China, Max-Planck-Institute for Chemical Physics of Solids, and Department of Materials Science and Engineering, College of Materials, Xiamen University

Received May 6, 2008. Revised Manuscript Received June 6, 2008

A family of lamellar mesostructured *n*-alkylamine borophosphates, denoted C_nA-BPO (BPO stands for inorganic borophosphate layer; $n = 9-15$, the number of carbon atoms in the *n*-alkylamine chain) has been prepared hydrothermally at 160 °C by using neutral *n*-alkylamines as templates. Those C_nA-BPO compounds were characterized by powder X-ray diffraction (XRD), Fourier transform infrared spectroscopy (FT-IR), thermogravimetric measurements, and differential thermal analysis (TG-DTA) as well as chemical analyses. Interestingly, these compounds may form a bilayer, a monolayer, or mixed state of bilayer and monolayer structures depending on the content of *n*-alkylamine. Linear relationships for both bilayer and monolayer compounds were observed between the interlayer distances and the numbers of carbon atoms in the *n*-alkylamine chain. The thickness of the inorganic layers, the arrangement of *n*-alkylamine in the interlayer space, and the composition of the compounds are proposed.

1. Introduction

Inorganic−organic hybrids are interesting materials not only for their structures, which exhibit a combination of the properties of organic materials with those of inorganic materials, but also for their potential applications in heterogeneous catalysis, photoluminescence, gas separation, and storage.[1,2] The self-assembly of hybrid inorganic−organic materials has flexibility in choosing organic, inorganic, or hybrid building blocks, which allows one to control the properties of materials and to optimize them for each desired application.[3–6]

Boron phosphate (BPO_4) belongs to the group of SiO_2-derivative structures and is well known as a solid acid used as an effective catalyst for a range of organic chemical reactions including hydration, dehydration, oligomerization, and isomerization.[7–12] Extensive work was devoted to increasing its surface-to-volume ratio.[13] Furthermore, BPO_4 also has specific applications as an optical material.[14–17] However, organic long-chain alkylamines have been widely used in synthesizing materials with alternating inorganic and organic layer structures by intercalating layered oxides such as silicates, transition-metal oxides, hydroxides, phosphates, arsenates, and even large borophosphate cluster anions.[18–23] Besides intercalation, *n*-alkylamines may also be used as templates to synthesize lamellar compounds by way of self-assembly.[24] A series of *n*-alkylamine dihydrogen phosphates $[C_nH_{2n+1}NH_3][H_2PO_4]$ was largely investigated as a type of compounds exhibiting reproducible ferroelastic switching.[25–29] Ozin et al. reported the synthesis of lamellar aluminophosphates using *n*-alkylamine dihydrogen phosphates or *n*-alkylamine monohydrogen phosphates as a surfactant and later on the transformation of a linear chain alumiophosphate to chain, layer, and framework structures.[30–36]

* Corresponding author. Tel: +86 21 52412073. Fax: +86 21 52413122. E-mail: jtzhao@mail.sic.ac.cn.

† Shanghai Institute of Ceramics, Chinese Academy of Sciences.

‡ Graduate School of the Chinese Academy of Sciences.

§ Max-Planck-Institute for Chemical Physics of Solids.

|| Xiamen University.

(1) Rao, C. N. R.; Cheetham, A. K.; Thirumurugan, A. *J. Phys.: Condens. Matter* **2008**, *20*, 083202.

(2) Cheetham, A. K.; Rao, C. N. R.; Feller, R. K. *Chem. Commun.* **2006**, 4780–4795.

(3) Byrd, H.; Pike, J. K.; Talham, D. R. *Chem. Mater.* **1993**, *5*, 709–715.

(4) Sellinger, A.; Weiss, P. M.; Nguyen, A.; Lu, Y.; Assink, R. A.; Gong, W.; Brinker, C. J. *Nature* **1998**, *394*, 256–260.

(5) Stein, A.; Melde, B. J.; Schroden, R. C. *Adv. Mater.* **2000**, *12*, 1403–1419.

(6) Hagrman, P. J.; Zubieta, J. *Inorg. Chem.* **2001**, *40*, 2800–2809.

(7) Otsuka, K.; Uragami, Y.; Hatano, M. *Catal. Today* **1992**, *13*, 667–672.

(8) Uragami, Y.; Otsuka, K. *J. Chem. Soc., Faraday Trans.* **1992**, *88*, 3605–3610.

(9) Tada, A.; Suzuka, H.; Imizu, Y. *Chem. Lett.* **1987**, *2*, 423–424.

(10) Gao, S.; Moffat, J. B. *J. Catal.* **1998**, *180*, 142–148.

(11) Imamura, S.; Higashihara, T.; Jindai, H. *Chem. Lett.* **1993**, *10*, 1667–1670.

(12) Imamura, S.; Higashihara, T.; Utani, K. *Ind. Eng. Chem. Res.* **1995**, *34*, 967–970.

(13) Satoshi, S.; Mitsuharu, H.; Toshiaki, S.; Fumio, N. *Bull. Chem. Soc. Jpn.* **1991**, *64*, 516–522.

(14) Schmidt, M.; Ewald, B.; Prots, Y.; Cardoso-Gil, R.; Armbruster, M.; Loa, I.; Zhang, L.; Huang, Y. X.; Schwarz, U.; Kniep, R. *Z. Anorg. Allg. Chem.* **2004**, *630*, 655–662.

(15) Li, Z. H.; Wu, Y. C.; Fu, P. Z.; Pan, S. L.; Chen, C. T. *J. Cryst. Growth* **2004**, *270*, 486–490.

(16) Li, Z. H.; Lin, Z. H.; Wu, Y. C.; Fu, P. Z.; Wang, Z. Z.; Chen, C. T. *Chem. Mater.* **2004**, *16*, 2906–2908.

(17) Lin, C. K.; Luo, Y.; You, H.; Quan, Z.; Zhang, J.; Fang, J.; Lin, J. *Chem. Mater.* **2006**, *18*, 458–464.

(18) Clearfield, A. *Chem. Mater.* **1998**, *10*, 2801–2810.

(19) Clearfield, A. *Prog. Inorg. Chem.* **1998**, *47*, 371–510.

(20) Han, Y. S.; Park, I.; Choy, J. H. J. *Mater. Chem.* **2001**, *11*, 1277–1282.

(21) Chen, D.; Sugahara, Y. *Chem. Mater.* **2007**, *19*, 1808–1815.

(22) Tahara, S.; Ichikawa, T.; Kajiwara, G.; Sugahara, Y. *Chem. Mater.* **2007**, *19*, 2352–2358.

(23) Do, J.; Jacobson, A. J. *Chem. Commun.* **2001**, *13*, 2436–2440.

(24) Chen, Z.; Loo, B. H.; Ma, Y.; Cao, Y.; Ibrahim, A.; Yao, J. *ChemPhysChem* **2004**, *5*, 1020–1026.

(25) Kroupa, J.; Fuith, A. *Phys. Rev. B* **1993**, *48*, 4119–4121.

(26) Waskowska, A. *Acta Crystallogr.* **1995**, *C51*, 420–423.

(27) Kasatani, H.; Iwata, M.; Terauchi, H.; Ishibashi, Y. *Ferroelectrics* **1999**, *229*, 255–260.

(28) Fabry, J.; Petricek, V.; Cisarova, I.; Kroupa, J. *Acta Crystallogr.* **1997**, *B53*, 272–279.

(29) Fabry, J.; Petricek, V.; Kroupa, J.; Cisarova, I. *Acta Crystallogr., Sect. B: Struct. Sci* **2000**, *56*, 906–914.

(30) Oliver, S.; Kuperman, A.; Coombs, N.; Lough, A.; Ozin, G. A. *Nature* **1995**, *378*, 47–50.

(31) Oliver, S.; Kuperman, A.; Lough, A.; Ozin, G. A. *Chem. Commun.* **1996**, 1761–1762.

(32) Ozin, G. A.; Oliver, S. *Adv. Mater.* **1995**, *7*, 943–947.

10.1021/la801403s CCC: $40.75 © 2008 American Chemical Society
Published on Web 07/22/2008

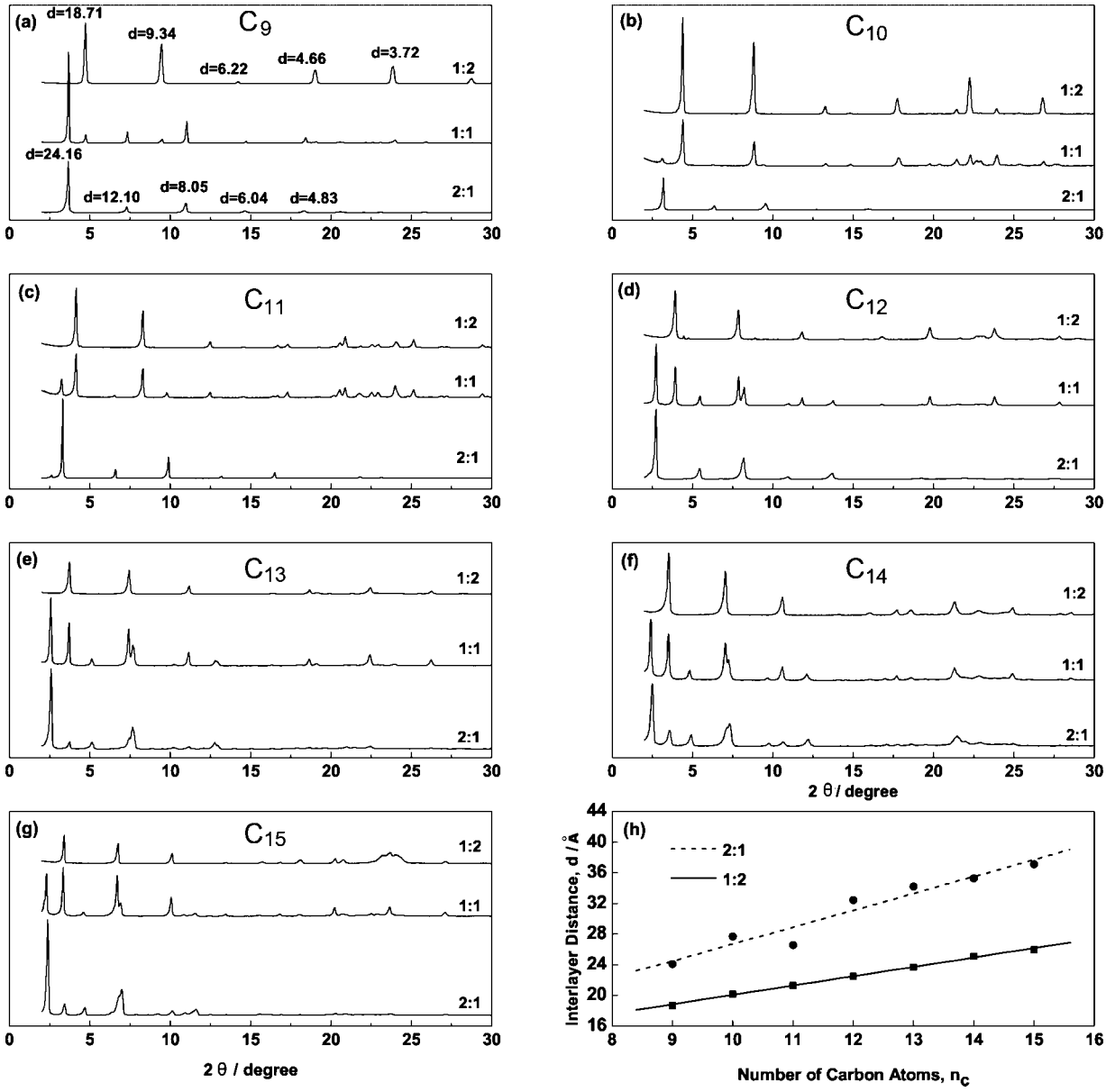

Figure 1. XRD patterns of C_nA-BPO with different *n*-alkylamine contents: (a) C_9A-BPO, (b) C_{10}A-BPO, (c) C_{11}A-BPO, (d) C_{12}A-BPO, (e) C_{13}A-BPO, (f) C_{14}A-BPO, and (g) C_{15}A-BPO. (h) Interlayer distances of C_nA-BPO as functions of the number of carbon atoms n_C.

Following this line, here we describe the assembly of $[PO_4]^{3-}$ or $[H_2PO_4]^-$ and $[B(OH)_4]^-$ anions using *n*-alkylamine cations to form a series of lamellar compounds C_nA-BPO with alternating inorganic and organic layers.

2. Experimental Section

2.1. Synthesis of *n*-Alkylamine Borophosphates. The syntheses of *n*-alkylamine borophosphates (herein expressed as C_nA-BPO) were carried out in Teflon-lined stainless-steel autoclaves ($V = 15$ mL) using H_3BO_3, H_3PO_4, *n*-alkylamine ($n = 9-15$), and distilled water as starting materials, with a filling degree of 80%. H_3BO_3 (3 mmol) and H_3PO_4 (85 wt%, 3 mmol) were first dispersed in 12 mL of distilled water with continuous stirring, followed by the addition of the necessary amount of *n*-alkylamine. To reach 2:1, 1:1, 1:2, and 1:4 molar ratios of C_nA/BPO, 6, 3, 1.5, and 0.75 mmol *n*-alkylamine were used accordingly. The reactants were homogenized under constant magnetic stirring before they were placed into autoclaves. After a reaction time of 5 days under autogenous pressure at 160 °C, the autoclaves were cooled to room temperature. The products were separated by ultrasonication and filtration, washed with warm water (40 °C) and ethanol several times until residual *n*-alkylamine and other soluble products were completely removed, and then dried in air at 50 °C for 12 h. The final white products were used in further characterizations.

Table 1. Summary of Interlayer Distances Obtained from XRD Data of C_nA-BPO with Different *n*-Alkylamine Content

	d_{100} Å			
$C_nH_{2n+1}NH_2$	2:1	1:1	1:2	1:4
C_9H_{19}	24.16	24.11 18.63	18.71	
$C_{10}H_{21}$	27.76	28.30 20.07	20.15	
$C_{11}H_{23}$	26.64	27.25 21.34	21.33	
$C_{12}H_{25}$	32.48	32.44 22.52	22.53	22.52
$C_{13}H_{27}$	34.24 23.74	34.52 23.88	23.74	
$C_{14}H_{29}$	35.32 24.66	36.78 25.23	25.09	
$C_{15}H_{31}$	37.11 25.82	38.44 26.45	26.00	

(33) Oliver, S.; Ozin, G. A.; Ozin, L. A. *Adv. Mater.* **1995**, *7*, 948–951.
(34) Oliver, S.; Coombs, N.; Ozin, G. A. *Adv. Mater.* **1995**, *7*, 931–935.
(35) Oliver, S.; Lough, A. J.; Ozin, G. A. *Inorg. Chem.* **1998**, *37*, 5021–5028.
(36) Oliver, S.; Kuperman, A.; Ozin, G. A. *Angew. Chem., Int, Ed.* **1998**, *37*, 46–62.

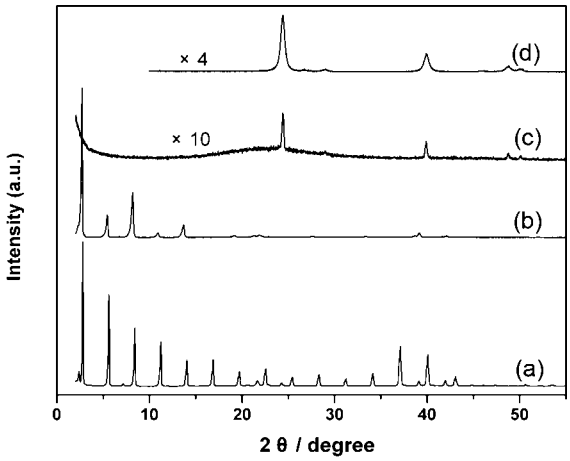

Figure 2. XRD patterns of (a) pure dodecylamine $C_{12}A$, (b) bilayer $C_{12}A$-BPO, (c) bilayer $C_{12}A$-BPO after treatment at 300 °C in air for 10 h, and (d) bilayer $C_{12}A$-BPO after treatment at 800 °C in air for 10 h.

2.2. Characterizations. Powder X-ray diffraction patterns (XRD) were collected at ambient temperature with a Rigaku D/max2500 diffractometer (Cu Kα radiation, 40 kV/200 mA). The interlayer distances of the compounds were determined on the basis of [001] reflections. Thermogravimetric analysis (TG) and differential thermal analysis (DTA) curves were recorded at a heating rate of 10 °C/min in flowing air with an STA 429C simultaneous thermal analyzer (Netzsch, Germany). Fourier transform infrared spectroscopy (FT-IR) was carried out on a Nexus FT-IR spectrometer (Thermo Nicolet). Elemental analyses of C and N were conducted on a PE 2400 II CHNS/O analyzer.

3. Results and Discussion

In Figure 1a−g, the XRD patterns of reaction products C_nA-BPO are depicted. Take C_9A-BPO as an example (Figure 1a), when C_nA/BPO = 2:1 and 1:2 (abbreviated 2:1 and 1:2 in the following text) and the ratios of *d* spacings for the first five peaks are all close to 1:1/2:1/3:1/4:1/5. Accordingly, they may be indexed as (00*l*) for a lamellar arrangement with periodic spacings of about 24.16 Å (2:1) or 18.17 Å (1:2), respectively. However, in the case of a 1:1 compound, it is interesting that the observed spacings can be divided into two distinct groups showing interlayer distances close to the values of the 2:1 and 1:2 phases, respectively. The product formed at a 1:1 ratio should be considered to be a mixture of 2:1 and 1:2 phases. This phenomena and the layered nature can also be observed in all the other products. The interlayer distances from the [00*l*] reflections of each product are presented in Table 1. The compounds from C_9A to $C_{12}A$ (2:1) and all of the 1:2 compounds were obtained as single phases, but the single phases of 2:1 products from $C_{13}A$ to $C_{15}A$ (Figure 1e−g) could not be obtained under this reacting situation. For $C_{13}A$ to $C_{15}A$, two interlayer distances are shown, and through the intensity of their reflection peaks, it can be seen that the unobtained 2:1 phase is the main phase with the 1:2 phase as a minor phase. So for the 2:1 composition of $C_{13}A$, $C_{14}A$, and $C_{15}A$ we used spacings of 34.24, 35.32, and 37.11 Å for the following calculation. The results of the calculation below also show that this choice is reasonable. The relationship between the interlayer distance, *d*, and the number of carbon atoms in the *n*-alkylamine chain, n_C, is demonstrated in Figure 1h, where two linear relationships are clearly observed, as expressed by $d = 2.2n_C + 4.71$ (2:1) and $d = 1.2n_C + 7.87$ (1:2). It demonstrates that the interlayer distances of the products increase with an increase in the number of carbon atoms in the *n*-alkylamine chain, with $C_{11}A$ (2:1) as an exception, which will be explained below.

Furthermore, when $C_{12}A$-BPO was heated to 300 °C in air for 10 h, the XRD pattern indicated the formation of BPO_4 (Figure 2c). The final decomposition product obtained by heating the material to 800 °C in air for 10 h was determined by XRD to be pure BPO_4 (Figure 2d). The XRD pattern of pure $C_{12}A$ (Figure 2a) with an interlayer distance of 31.35 Å and an XRD pattern of $C_{12}A$-BPO (2:1) with an interlayer distance of 32.48 Å (Figure 2b) are also given in the picture as references. It is reasonable to deduce that the existence of the inorganic layer and the observed interlayer distance are determined by the packing of the inorganic borophosphate layers with the *n*-alkylamine cations in the interlayer space. The diffraction peaks of BPO_4 did not show in the XRD pattern of $C_{12}A$-BPO, which indicates an inorganic−organic composite mesolamellar phase lacking long-range order within the inorganic layer regions of the structure.[30] In the inorganic layer, tetrahedral B and P centers are connected through bridging oxygens, just like the layered aluminophosphates containing interlamellar cyclohexylamine,[31] but the crystalline phase of BPO_4 did not form.

Consider that two types of chain arrangement can lead to the same interlayer height ((a) tilted, all-trans chains and (b) chains with numerous gauche conformers), so to confirm the configuration of *n*-alkylamine in the compounds, we studied the FT-IR spectra of $C_{12}A$-BPO with different $C_{12}A$ contents. Figure 3 demonstrates the selected FT-IR spectra of $C_{12}A$-BPO: (a) 2:1, (b) 1:2, and (c) 1:4. According to the database of the ChemExper Chemical Directory (http://search.acros.com/), the characteristic infrared spectral peaks at 720, 1469, 2850, and 2918 cm^{-1} correspond to dodecylamine $C_{12}A$; the peak at 1558 cm^{-1} is the symmetric bend of NH_3, and 2956 cm^{-1} is attributed to the asymmetric stretching vibration of CH_3.[37] The group of bands in the range of 1045−1150 cm^{-1} are due to the asymmetric stretching vibrations in the $[PO_4]^{3-}$ tetrahedron, and the peaks at 540.3 and 960.4 cm^{-1} belong to pseudolattice translations of B−O;[38] this also confirms the possible presence of $[B(OH)_4]$, $[PO_4]$, and $[H_2PO_4]$ anions.

It is well known that the positions of the antisymmetric stretching band (2920 cm^{-1}) and the symmetric stretching band (2850 cm^{-1}) of CH_2 groups (abbreviated $\nu_{as}(CH_2)$ and $\nu_s(CH_2)$, respectively) in *n*-alkylamine chains are sensitive to chain conformation and that these two bands shift to higher wavenumbers if disorder is introduced into the *n*-alkylamine chains.[39] In the selected range of 2700−3100 cm^{-1}, all of the spectra exhibit four major absorptances. In the FT-IR spectra of $C_{12}A$-BPO (2:1), the $\nu_{as}(CH_2)$ band and the $\nu_s(CH_2)$ band are observed at 2918 0.1 and 2850.3 cm^{-1}, and these band positions correspond to an all-trans conformation. In the case of 1:2, the $\nu_{as}(CH_2)$ band and the $\nu_s(CH_2)$ band are observed at 2925.5 and 2851.8 cm^{-1}, and these band positions correspond to the disordered gauche structure. To confirm our opinion, the 1:4 composition product was synthesized, and its stretching bands are observed at 2926.1 and 2852.3 cm^{-1}, which means that the conformation of dodecylamine is more disordered than that of the 1:2 structure. Thus, in $C_{12}A$-BPO, as the amount of dodecylamine increases, the wavenumber of $\nu_{as}(CH_2)$ gradually decreases to 2918.1 cm^{-1}, indicating that the dodecylamine chains in $C_{12}A$-BPO become more ordered and closer packed.

Here we propose the existence of two types—bilayer C_nA-BPO (Scheme 1a) and monolayer C_nA-BPO (Scheme 1b) with

(37) Paivarinta, J.; Karlsson, S.; Poso, A.; Hotokka, M. *Chem. Phys.* **2001**, *263*, 127–138.

(38) Adamczyk, A.; Handke, M. *J. Mol. Struct.* **2000**, *555*, 159–164.

(39) Vaia, R. A.; Teukolsky, R. K.; Giannelis, E. P. *Chem. Mater.* **1994**, *6*, 1017–1022.

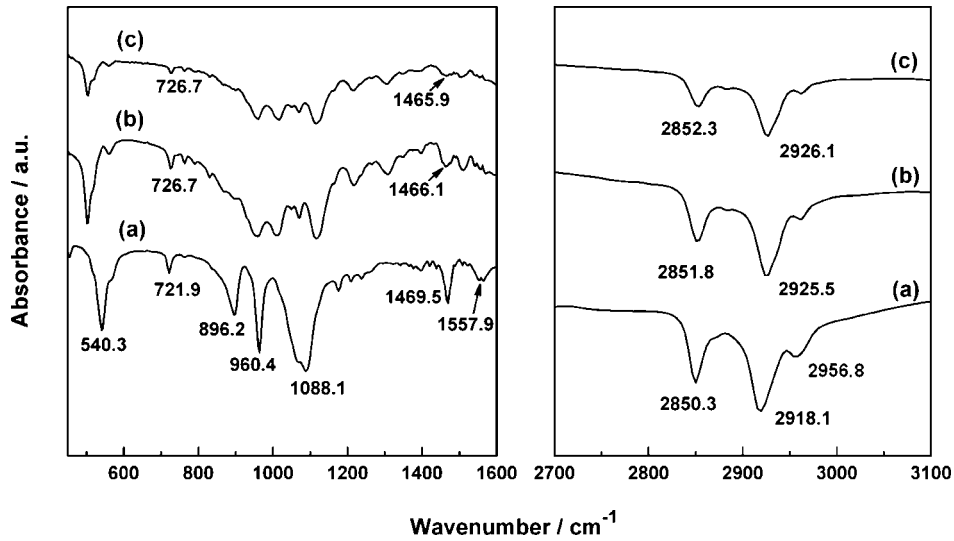

Figure 3. Selected regions of the FT-IR spectra of the (a) C_{12}A-BPO bilayer with 2:1 C_{12}A content, (b) C_{12}A-BPO monolayer with 1:2 C_{12}A content, and (c) C_{12}A-BPO monolayer with 1:4 C_{12}A content.

Scheme 1. Computer models of the *n*-alkylamine borophosphate (here we take $n = 12$ as an example): (a) biolayer C_{12}A-BPO with tilted, all-trans chains, (b) monolayer C_{12}A-BPO with numerous gauche chains, (c) combination of an inorganic layer and *n*-alkylamine through hydrogen bonding in the case of a bilayer, and (d) combination of an inorganic layer and *n*-alkylamine through hydrogen bonding in the case of a monolayer

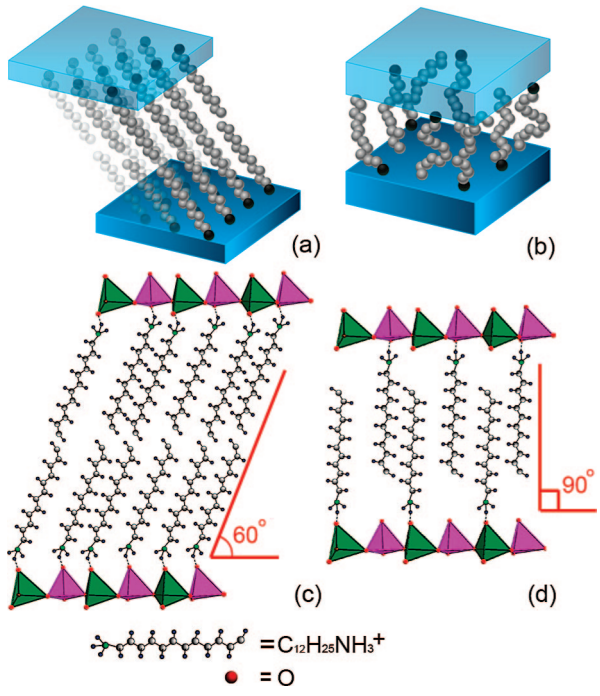

different interlamellar arrangements—depending on the n_C value and the content of *n*-alkylamine. In the case of bilayer C_nA-BPO, the configuration of *n*-alkylamine between the inorganic layers possesses an all-trans conformation. In the case of the C_nA-BPO monolayer, the configuration of *n*-alkylamine between the inorganic layers possesses a disordered gauche structure. A further explanation of the two structures is as follow.

In the trans−trans conformation, it is estimated to be 1.27 Å for each additional carbon atom, and it is reasonable to assume that the amine is present in the compounds as a bimolecular layer

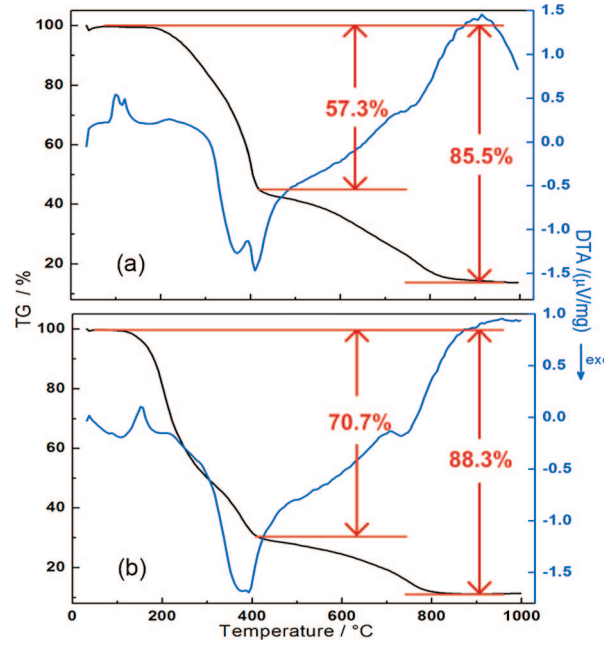

Figure 4. TG-DTA curves of (a) monolayer C_{12}A-BPO and (b) bilayer C_{12}A-BPO.

Table 2. Calculated and Observed C and N Element Contents (wt %) of C_{12}A-BPO and Overall Weigh Losses for Both the Bilayer and Monolayer

	C (wt %)		N (wt %)		overall weight loss (wt %)	
	calcd	obsd	calcd	obsd	calcd	obsd
bilayer	62.7	61.6	6.1	5.7	88.4	88.3
monolayer	52.5	50.5	5.1	4.6	80.7	85.5

of extended molecules when the slope of the straight line defining the interlayer distances is higher than 1.27 Å. When the value is lower than 1.27 Å, the arrangement can be a monolayer.[40] So in the case of 2:1, the mean increment of the interlayer distance ($\Delta d/\Delta n_C$) is 2.2 Å (according to the mentioned relationship $d = 2.2n_C + 4.71$), and this value corresponds to a tilted bilayer arrangement of *n*-alkylamine chains in the interlayer space of

(40) Menendez, A.; Barcena, M.; Jaimez, E.; Garcia, J. R.; Rodriguez, J. *Chem. Mater.* **1993**, *5*, 1078–1084.

inorganic BPO. The tilt angle of the *n*-alkylamine chains with respect to the surface of the inorganic BPO layer is calculated to be arcsin(2.2/1.27 × 2) = 60°, where 1.27 Å is the length increment per carbon atom in a linear all-trans chain. Anyway, the value of the tilt angle indicates that the N−C bond is not strictly perpendicular to the layers (53.8° for a perpendicular arrangement).

As for the 1:2 compound, the increasing of 1.2 Å (according to $d = 1.2n_C + 7.87$) per carbon atom implies monolayer arrangements of the *n*-alkylamine cations between the layers. However, we can also note the change in interlayer distance when going from an n_C to and n_{C+1} compound, which depends on whether n_C is even or odd. Assuming the N−C bond to be perpendicular to the layer, tetrahedral bond angles of 109° 21′, and a C−C bond length of 1.54 Å, alternating small and large changes in the interlayer distances can be estimated as follow: $d(n_{C+1}) - d(n_C)$ for *n*-alkylamine bilayers is expected to be 1.02 Å (n_C is odd) and 3.08 Å (n_C is even), and for *n*-alkylamine monolayers, it is 0.51 and 1.54 Å for odd and even n_C values, respectively. However, in our case no odd−even alteration is apparent in monolayer C_nA-BPO, which also illustrates that there is disorder in the monolayer and the chain orientation in it is 90°. Furthermore, the value of the interlayer distance of a hypothetic *n*-alkylamine without carbon atoms ($n = 0$) may be used to estimate the region occupied by the inorganic layer and the terminal $-NH_3^+$ groups. Therefore, assuming the $-NH_3^+$ group to be independent of *n*, according the obtained relationships $d = 2.2n_C + 4.71$ and $d = 1.2n_C + 7.87$, it can be estimated that the thicknesses of the inorganic layers are 4.71 Å for the bilayer and 7.87 Å for the monolayer, respectively. And by considering the packing of *n*-alkylamine in the bilayer to be more ordered and more compact compared to that in monolayer, the estimated thickness of the monolayer contains more space than that of the bilayer.

Furthermore, a proposed connection between *n*-alkylamine and inorganic layer is shown in Scheme 1c,d for the bilayer and monolayer, respectively. The reaction force is discussed as follows: H_3PO_4 and H_3BO_3 act as proton donors, and after the protonation of the $-NH_2$ groups, there is a tendency for the protonated $-NH_3^+$ to be distribute as widely as possible in the interlayer space; the combination of $-NH_3^+$ with the inorganic layer is through hydrogen bonding N−H···O. At the same time, there is a tendency for the apolar alkylamine chains to interact with each other by van der Waals' interactions in the case of the bilayer; as for the monolayer with lower *n*-alkylamine content, the chains tends to cross each other to form a monolayer in the case of enough interlayer space. In fact, the abrupt slope decrease at $n_C = 11$ may be explained as follow: with increasing *n*-alkylamine length, the van der Waals' interactions also increase, which should result in a more ordered arrangement,[23] giving rise to a decrease in the interlayer distance compared to that for C_{10}A-BPO.

TG-DTA curves taken in air flow at a heating rate of 10 °C/min are shown in Figure 4. Bilayer C_{12}A-BPO begins to decompose at about 140 °C; monolayer C_{12}A-BPO is more stable because its weight remains constant until 200 °C, where decomposition begins. This observation also confirms that the combination of NH_3^+ and the inorganic layer is more stable than the van der Waals interactions between *n*-alkylamine chains. Monolayer C_{12}A-BPO and bilayer C_{12}A-BPO act the same way when the temperature is higher than 400 °C. The weight losses of the main stages are shown in the Figures. The first stage (under 400 °C) is considered to be the liberation of C_{12}A and the formation of H_2O molecules through dehydration of the protonated $-NH_3^+$ and OH^- in the inorganic layer. The second stage (above 400 °C) is associated with the further dehydration of the hydrated borophosphate layer to form BPO_4. In accordance with this analysis, bilayer C_{12}A-BPO and monolayer C_{12}A-BPO have compositions close to $[C_{12}H_{25}NH_3]_4[B(OH)_4][PO_4]$ and $[C_{12}H_{25}NH_3]_2[B(OH)_4][H_2PO_4]$, respectively. The overall weight loss, the amounts of C and N observed through chemical analyse,s and the value calculated from the supposed composition are listed in Table 2. We can see that the observed contents of C and N are close to the calculated value. In the case of the bilayer, the overall observed weight loss (88.3%) is in good agreement with the value of 88.4% calculated for the composition, and as for the monolayer, the overall observed weight loss of 85.5% is close to calculated 80.7%. In addition, we can deduce a structure similar to that of an inorganic monolayer through the stoichiometry. In the case of the bilayer, $[BO_4]$ and $[PO_4]$ link to each other through two of their four vertexes and the other two vertexes link to *n*-alkylamine, so the four vertexes are all occupied. But in the case of a monolayer, only one *n*-alkylamine links to one vertex of the tetrahedral, so there is still one free vertex. Because of this free vertex, it may link to some other $[BO_4]$ or $[PO_4]$ tetrahedral. As a result, the monolayer is thicker than the bilayer.

4. Conclusions

A family of lamellar mesostructured *n*-alkylamine borophosphates (C_nA-BPO, $n = 9-15$) was synthesized and investigated. The interlayer distances of the compounds versus the number of carbon atoms (n_C) in the *n*-alkylamine chain of the amine indicates that amine molecules were packed in the interlamellar space either as a bilayer (*d* spacing 24.16 to 37.11 Å) or as an intercrossing monolayer (*d* spacing 18.71 to 26.00 Å), depending on the ratio of C_nA/BPO. The thicknesses of the inorganic layers are to be 4.71 Å for the bilayer and 7.87 Å for the monolayer. The FT-IR spectra of the compounds with *n*-alkylamine clearly show that *n*-alkylamine chains possess an all-trans conformation with a high content of *n*-alkylamine and a disorder (kink and gauche blocks) conformation with a low content of *n*-alkylamine. The composition of C_{12}A-BPO is close to $[C_{12}H_{25}NH_3]_4[B(OH)_4][PO_4]$ in the case of the bilayer and $[C_{12}H_{25}NH_3]_2[B(OH)_4][H_2PO_4]$ in the case of the monolayer. In conclusion, we have demonstrated that well-ordered lamellar mesostructured phases can be obtained from inorganic cluster anions and *n*-alkylamine cations. It is believed that a similar strategy could be applicable to the synthesis of novel mesostructured phases, and it is possible to get different interlayer spacings with different *n*-alkylamines and different contents. The inorganic mesostructured borophosphates pillared with functional molecules will be interesting materials in various applications, such as heterogeneous catalysis and as specific adsorbents.

Acknowledgment. This work was supported by the Key Project (50332050) from the NNSF of China and the State 973 project (2007CB936704), the Hundred Talents Program of the Chinese Academy of Sciences, and the fund for Young Leading Researchers from the Shanghai Municipal Government.

LA801403S